J|A|C|S
ARTICLES

Published on Web 04/09/2008

Structural, Optical, and Electrical Properties of PbSe Nanocrystal Solids Treated Thermally or with Simple Amines

Matt Law,* Joseph M. Luther, Qing Song, Barbara K. Hughes, Craig L. Perkins, and Arthur J. Nozik*

National Renewable Energy Laboratory, Golden, Colorado 80401

Received January 3, 2008; E-mail: matt_law@nrel.gov; arthur_nozik@nrel.gov

Abstract: We describe the structural, optical, and electrical properties of films of spin-cast, oleate-capped PbSe nanocrystals that are treated thermally or chemically in solutions of hydrazine, methylamine, or pyridine to produce electronically coupled nanocrystal solids. Postdeposition heat treatments trigger nanocrystal sintering at ~200 °C, before a substantial fraction of the oleate capping group evaporates or pyrolyzes. The sintered nanocrystal films have a large hole density and are highly conductive. Most of the amine treatments preserve the size of the nanocrystals and remove much of the oleate, decreasing the separation between nanocrystals and yielding conductive films. X-ray scattering, X-ray photoelectron and optical spectroscopy, electron microscopy, and field-effect transistor electrical measurements are used to compare the impact of these chemical treatments. We find that the concentration of amines adsorbed to the NC films is very low in all cases. Treatments in hydrazine in acetonitrile remove only 2−7% of the oleate yet result in high-mobility *n*-type transistors. In contrast, ethanol-based hydrazine treatments remove 85−90% of the original oleate load. Treatments in pure ethanol strip 20% of the oleate and create conductive *p*-type transistors. Methylamine- and pyridine-treated films are also *p*-type. These chemically treated films oxidize rapidly in air to yield, after short air exposures, highly conductive *p*-type nanocrystal solids. Our results aid in the rational development of solar cells based on colloidal nanocrystal films.

Introduction

Thin films of semiconductor nanocrystals (NCs) are emerging as an important class of materials for electronic and optoelectronic devices such as field-effect transistors,[1–7] photodetectors,[8–11] light-emitting diodes,[12–16] metamaterials,[17–19] and solar cells.[20,21] Reliable synthetic routes to high-quality colloidal NCs of controlled size and shape now exist for most binary and some ternary semiconductors.[22] The ready availability of NCs, combined with their unique features (bandgap tunability, multiple exciton generation,[23,24] self-assembly) and the promise of inexpensive device fabrication (by drop casting, spin coating, printing[25] or spraying[26]), drives the development of NC-based optoelectronic technologies. Offsetting these advantages are several difficulties inherent to NC building blocks, including their metastability, nonzero charging energies, susceptibility to oxidization, and sensitivity to surface states. Nanocrystals are generally hard to dope in a controlled fashion.[27] Furthermore, colloidal NCs typically possess electrically insulating organic ligand shells that must be shortened or removed to convert NC solids from insulators to conductors. Postdeposition thermal or

(1) Ridley, B. A.; Nivi, B.; Jacobson, J. M. *Science* **1999**, *286*, 746.
(2) Morgan, N. Y.; Leatherdale, C. A.; Jarosz, M. V.; Drndić, M.; Kastner, M. A.; Bawendi, M. *Phys. Rev. B* **2002**, *66*, 075339.
(3) Yu, D.; Wang, C.; Guyot-Sionnest, P. *Science* **2003**, *300*, 1277.
(4) Talapin, D. V.; Murray, C. B. *Science* **2005**, *310*, 86.
(5) Kim, H.; Cho, K.; Kim, D.-W.; Lee, H.-R.; Kim, S. *Appl. Phys. Lett.* **2006**, *89*, 173107.
(6) Porter, V. J.; Mentzel, T.; Charpentier, S.; Kastner, M. A.; Bawendi, M. G. *Phys. Rev. B* **2006**, *73*, 155303.
(7) Urban, J. J.; Talapin, D. V.; Shevchenko, E. V.; Kagan, C. R.; Murray, C. B. *Nat. Mater.* **2007**, *6*, 115.
(8) Ginger, D. S.; Greenham, N. C. *J. Appl. Phys.* **2000**, *87*, 1361.
(9) Jarosz, M. V.; Porter, V. J.; Fisher, B. R.; Kastner, M. A.; Bawendi, M. G. *Phys. Rev. B* **2004**, *70*, 195327.
(10) Oertel, D. C.; Bawendi, M. G.; Arango, A. C.; Bulović, V. *Appl. Phys. Lett.* **2005**, *87*, 213505.
(11) Konstantatos, G.; Howard, I.; Fischer, A.; Hoogland, S.; Clifford, J.; Klem, E.; Levina, L.; Sargent, E. H. *Nature* **2006**, *442*, 180.
(12) Colvin, V. L.; Schlamp, M. C.; Alivisatos, A. P. *Nature* **1994**, *370*, 354.
(13) Artemyev, M. V.; Sperling, V.; Woggon, U. *J. Appl. Phys.* **1997**, *81*, 6975.
(14) Gao, M.; Lesser, C.; Kirstein, S.; Möhwald, H.; Rogach, A. L.; Weller, H. *J. Appl. Phys.* **2000**, *87*, 2297.
(15) Coe, S.; Woo, W.-K.; Bawendi, M.; Bulović, V. *Nature* **2002**, *420*, 800.
(16) Bertoni, C.; Gallardo, D.; Dunn, S.; Gaponik, N.; Eychmüller, A. *Appl. Phys. Lett.* **2007**, *90*, 034107.
(17) Redl, F. X.; Cho, K.-S.; Murray, C. B.; O'Brien, S. *Nature* **2003**, *423*, 968.
(18) Shevchenko, E. V.; Talapin, D. V.; Kotov, N. A.; O'Brien, S.; Murray, C. B. *Nature* **2006**, *439*, 55.
(19) Shevchenko, E. V.; Talapin, D. V.; Murray, C. B.; O'Brien, S. *J. Am. Chem. Soc.* **2006**, *128*, 3620.
(20) Nozik, A. J. *Physica E* **2002**, *14*, 115.
(21) Gur, I.; Fromer, N. A.; Geier, M. L.; Alivisatos, A. P. *Science* **2005**, *310*, 462.
(22) Yin, Y.; Alivisatos, A. P. *Nature* **2005**, *437*, 664.
(23) Schaller, R.; Klimov, V. *Phys. Rev. Lett.* **2004**, *92*, 186601.
(24) Ellingson, R. J.; Beard, M. C.; Johnson, J. C.; Yu, P.; Micic, O. I.; Nozik, A. J.; Shabaev, A.; Efros, A. L. *Nano. Lett.* **2005**, *5*, 865.
(25) Tekin, E.; Smith, P. J.; Hoeppener, S.; van den Berg, A. M. J.; Susha, A. S.; Rogach, A. L.; Feldmann, J.; Schubert, U. S. *Adv. Funct. Mater.* **2007**, *17*, 23.
(26) Pehnt, M.; Schulz, D. L.; Curtis, C. J.; Jones, K. M.; Ginley, D. S. *Appl. Phys. Lett.* **1995**, *67*, 2176.
(27) Erwin, S. C.; Zu, L.; Haftel, M. I.; Efros, A. L.; Kennedy, T. A.; Norris, D. J. *Nature* **2005**, *436*, 91.

10.1021/ja800040c CCC: $40.75

chemical treatments are popular for this purpose.[3,4,7,9,11,28] The latter involve replacing the long chain capping ligands with small molecules that can decrease the inter-NC spacing, passivate surface traps and chemically dope the films. Despite the frequent use of such thermal and chemical treatments in recent studies, there is at present little systematic understanding of their impact on the optical and electronic properties of NC solids.

Here we describe how various thermal treatments and amine-based chemical treatments affect the optical and electronic properties of spin-cast, oleic-acid-capped PbSe NC films. Electron microscopy, X-ray scattering, visible-infrared absorption spectroscopy, Fourier transform infrared spectroscopy, X-ray photoelectron spectroscopy, NMR, differential scanning calorimetry, and field-effect transistor measurements are used to understand the effects of these treatments on 50−450 nm thick films. We are interested in fabricating NC solids suited for use in novel solar cells, either as light-absorbing layers (e.g., films of IV−VI quantum dots exhibiting multiple exciton generation)[29] or as scaffolding for light absorbers (e.g., films of large band gap II−VI or III−V NCs in tandem dye-sensitized solar cells). These applications require high-quality, conductive NC films with thicknesses of 0.5−10 μm. In the former case, the capping ligands should be optimized for the creation of electron and hole minibands between the NCs. For use in dye-sensitized cells, the original ligand shell must be stripped to permit the adsorption of charge-transfer dye molecules on the clean NC surfaces.

Experimental Section

Materials. Lead oxide (99.999%), selenium (99.99%), oleic acid (technical grade, 90%), oleylamine (70%), 1-octadecene (ODE, 90%), diphenylphosphine (DPP, 98%), tetrachloroethylene (TCE, 99.9+%), methylamine (33 wt% in absolute ethanol) and anhydrous ethanol, hexane, chloroform, octane, pyridine, and hydrazine were purchased from Aldrich and used as received. Trioctylphosphine (TOP, technical grade, >90%) was acquired from Fluka. Anhydrous chloroform-*d* (98.8%, Aldrich) was used in NMR experiments.

PbSe Nanocrystal Synthesis. Standard air-free techniques were employed throughout. PbSe NCs were synthesized according to a modified literature procedure.[30,31] Briefly, 0.22 g of PbO was dissolved in a mixture of 0.73 g of oleic acid and 10 g of ODE at 150 °C to yield a clear solution. A mixture of 3 mL of 1 M TOP-Se and 28 mg of DPP was swiftly injected into the solution at 180 °C, and the temperature was reduced to 155−160 °C to allow the NCs to grow to the desired size. The reaction was then quenched in a water bath and diluted with 10 mL of hexane. The NCs were purified by precipitation twice with acetone/chloroform and once with ethanol/hexane and stored as a powder. The final NC yield is 50−60% (Pb basis).

Preparation of NC Films. All work was performed in a nitrogen glovebox. Depending on the experimental requirement, 1-in. polished sapphire windows, 1-cm double-side-polished *i*-Si(100) or 1.5-cm degenerately doped *p*-Si(100) with a 110-nm-thick oxide layer served as substrates for film deposition. Unless indicated, no effort was made to modify the hydrophobicity or chemical functionality of the substrates beyond cleaning them in acetone. PbSe NC films were spin cast from an octane solution with a concentration of 380 mg mL^{-1} (10 s @ 900 rpm, then 15 s @ 1200 rpm), yielding 450-nm-thick superlattice NC films with a peak-to-valley roughness of ±75 nm. Spinning NCs from TCE or chloroform resulted in films of poor quality (i.e., clumpy or cracked films with rough surfaces).

Thermal and Chemical Treatments. Thermal treatments of PbSe NC films were performed on a hot plate in a nitrogen glovebox (50 °C min^{-1} heating rate) without exposing the samples to air. For the chemical treatments, samples were immersed in 3−5 mL of hydrazine (N_2H_4), methylamine (CH_3NH_2), or pyridine (C_5H_5N) solutions (concentration and duration as indicated in the text) in capped glass vials with occasional gentle agitation, also air-free. After a prescribed soak time (usually 24 h), the samples were carefully removed from the vials, washed with clean solvent, and allowed to dry in the glovebox.

Film Characterization. Transmission electron microscopy (TEM) characterization was performed on an FEI Tecnai G^2 operating at 200 keV. A JEOL JSM-7000F field emission scanning electron microscope (SEM) was used to image the films. Film thicknesses measured by SEM were corroborated with a DekTak II profilometer. Small angle and wide angle X-ray scattering measurements (SAXS and WAXS) were carried out with a Scintag X1 diffractometer (Cu Kα radiation). In WAXS, the crystallite diameter was determined from the Scherrer equation for spherical particles, $d = (K_S\lambda)/(\beta_{2\theta} \cos \theta)$ with $K_S = (4/3)(\pi/6)^{1/3}$. In situ WAXS data were acquired on a Bruker D8 Discover diffractometer utilizing a polyetheretherketone (PEEK) sample dome. Optical absorption data were acquired with a Shimadzu UV-3600 spectrophotometer equipped with an integrating sphere. Fourier transform infrared (FTIR) data were taken on a Nicolet 510 FT-IR spectrometer. X-ray photoelectron spectroscopy (XPS) was performed using a modified Physical Electronics 5600 XPS using monochromatic Al Kα radiation and a pass energy of 29 eV. The films were found to charge slightly during analysis, so spectra were aligned by placing the Pb $4f_{7/2}$ peak at the lowest observed binding energy of 137.3 eV. The cluster tool to which the XPS system is attached allows the analysis of films without exposing them to air. Thermal analyses were carried out using a TA Instruments Q1000 differential scanning calorimeter (DSC) and a Q500 thermogravimetric analyzer (TGA). ^{1}H NMR spectra were acquired air-free in anhydrous $CDCl_3$ on a Varian INOVA-400 spectrometer.

For electrical studies, PbSe NC films were spin-cast onto degenerately doped silicon substrates coated with a 110-nm-thick thermal SiO_2 gate oxide. Source and drain electrodes (5 nm Ti/35 nm Au) spaced 10−50 μm apart were patterned onto the SiO_2 surface before nanocrystal deposition. When the postdeposition treatment caused significant film cracking, two rounds of nanocrystal deposition and treatment were used to prepare films largely free of through-film cracks. Electrical tape served to prevent contact between the NC film and the gate electrode during NC deposition. Field-effect measurements were performed in a glovebox with a homemade probe station using a Keithley 236 source-measure unit (source/drain) and a Keithley 230 programmable voltage source (gate) driven by Labview software. The noise limit of the setup was ~10 pA. Samples for Hall effect measurements were prepared on clean glass substrates and measured in air.

Results and Discussion

Nanocrystal Characterization. Typical TEM, optical absorption, and WAXS data for the PbSe nanocrystals used in this study are presented in Figure 1. The NCs are monodisperse rock salt cuboctahedra 6.5 ± 0.5 nm in diameter. WAXS peak fitting yields a slightly smaller average diameter (6 nm) compared to TEM (inset Figure 1b). Optical measurements show a first excitonic transition, $\lambda_{exciton}$, at 1896 nm (0.66 eV) for the NCs dispersed in TCE. We used several batches of NCs in this study, each with an average NC diameter in the range 6.5−8 nm ($\lambda_{exciton}$ = 1896−2050 nm). Spin coating from octane solutions yields NC superlattice films with a strong PbSe 220 texture in

(28) Murphy, J. E.; Beard, M. C.; Nozik, A. J. *J. Phys. Chem. B* **2006**, *110*, 25455.
(29) Luther, J. M.; Beard, M. C.; Song, Q.; Law, M.; Ellingson, R. J.; Nozik, A. J. *Nano Lett.* **2007**, *7*, 1779.
(30) Murphy, J. E.; Beard, M. C.; Norman, A. G.; Ahrenkiel, S. P.; Johnson, J. C.; Yu, P.; Mićić, O. I.; Ellingson, R. J.; Nozik, A. J. *J. Am. Chem. Soc.* **2006**, *128*, 3241.
(31) Steckel, J. S.; Yen, B. K. H.; Oertel, D. C.; Bawendi, M. G. *J. Am. Chem. Soc.* **2006**, *128*, 13032.

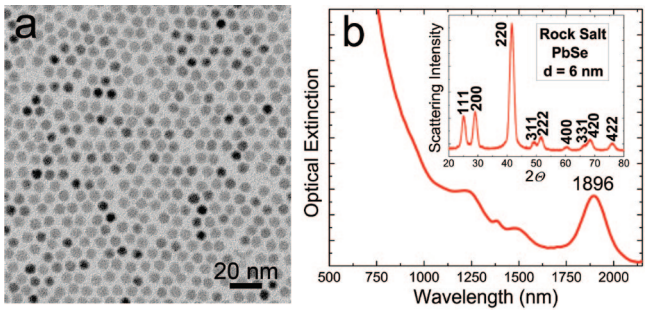

Figure 1. Basic characterization of the PbSe nanocrystals used in this study. (a) Low-resolution TEM. (b) Optical absorption spectrum of the NCs in TCE solution. The fwhm of the first exciton peak is 55 meV. Inset is the WAXS pattern of the NCs.

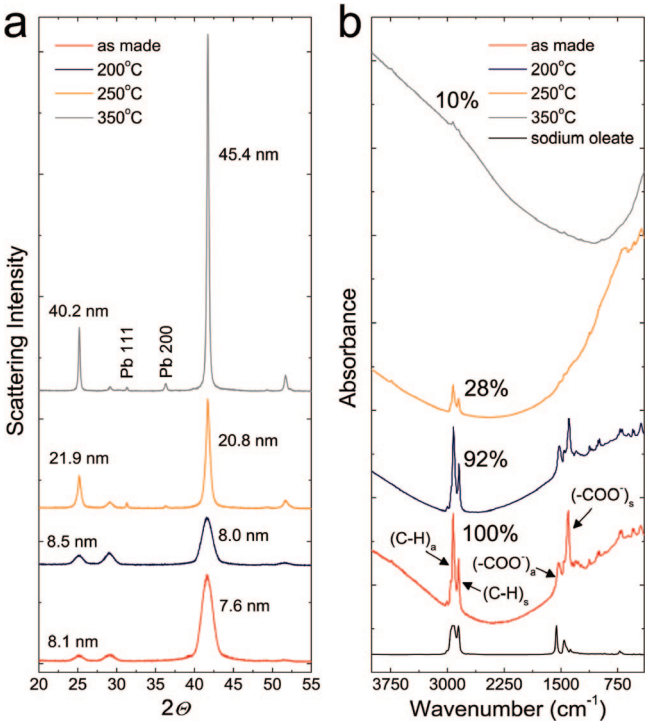

Figure 2. (a) WAXS patterns of PbSe NC films on sapphire substrates heated to 200, 250, and 350 °C. Crystalline Pb was detected with WAXS starting at 250 °C. Calculated average crystallite sizes for the 111 and 220 reflections are indicated. (b) FTIR spectra of samples on silicon substrates. A small amount of a diphenylphosphine (DPP) derivative is coadsorbed with oleate on the surface of the as-made films (out-of-plane C−H bends at 700−740 cm^{-1}, in-plane C−H bends at 990−1020 cm^{-1}). The integrated C−H stretch intensity, used to quantify the amount of oleate remaining on the films, is given as a percentage of the oleate loading of the as-made film. The sloping backgrounds are due to etaloning. A spectrum of sodium oleate is shown at the bottom for reference. These data were acquired with NCs having $\lambda_{exciton} = 2030$ nm. The samples were exposed to air during the measurement process.

WAXS patterns and multiple sharp reflections in SAXS patterns, similar to films made by Talapin and Murray[4] by drop casting (see Figures 2, 3, 7, and 8).

Thermal Treatments of PbSe NC Films. The NC films were heated to temperatures of up to 500 °C in a nitrogen-filled glovebox in an effort to remove the surface oleate, but the NCs were found to become thermally unstable at temperatures well below those required for oleate pyrolysis. Figure 2 presents ex situ WAXS patterns and FTIR spectra of films treated at 200, 250, and 350 °C for 1 h. WAXS peak fitting shows that the NCs begin to grow at ∼200 °C, tripling in diameter at 250 °C and sextupling at 350 °C. The growth is fairly isotropic and results in large spheroidal grains. Crystalline Pb appears at ∼250 °C, which suggests that selenium evaporation or segregation commences around this temperature. Meanwhile, the FTIR spectra show that the intensities of the C−H and COO^- stretches decrease as a function of temperature until essentially all of the oleate has been pyrolyzed by ∼350 °C, leaving behind an inorganic polycrystalline PbSe thin film. These data illustrate that thermal treatments are not able to remove a significant fraction of the oleate without causing NC growth and elemental segregation.

The sintering process was also monitored by optical absorption spectroscopy, SAXS, and SEM. Figure 3a shows that the energy of the first excitonic absorption broadens by 25 meV and red-shifts by 11 meV in response to the 200 °C treatment, which we attribute mainly to a slight growth of the NCs (see Figure 2a). Treatments at higher temperatures obliterate all of the excitonic features in the spectra because the NCs sinter and lose size monodispersity, making the films more like bulk polycrystalline PbSe.[32] The large red shift in absorption onset signals the occurrence of a Mott-type insulator to metal transition that is verified in DC electrical measurements (see below). Growth of the NCs also progressively destroys the superlattice order evident in SAXS patterns (Figure 3b). SEM imaging shows that the films densify and coarsen while sintering, losing about 50% of their volume during the 350 °C treatments (Figure 4).

The nanocrystals do not melt at these temperatures but rather ripen via solid-state surface diffusion.[33] In situ X-ray diffraction heating experiments directly show that the NCs grow without melting (Figure 5). Furthermore, there is no evidence for a PbSe crystallization event in DSC-TGA curves of samples cooled from 550 °C, the highest temperature explored in this study (Figure S1 in the Supporting Information). Considering the relatively large size of the NCs and the fairly high melting point of bulk PbSe (1067 °C), a size-induced melting point depression of this magnitude is unlikely. What is striking to us is the propensity of the PbSe NC films to sinter at such low temperatures. In contrast, ZnSe NCs of similar size did not increase in diameter during treatments at temperatures as high as 500 °C (not shown). It would be interesting to explore the reasons for the varied sintering behavior of the metal selenide NC films.

Electrical Measurements of Thermally-Treated Films. As-made PbSe NC films are highly insulating (with a conductivity of $<10^{-9}$ S cm^{-1}) and unresponsive to gate bias. The conductivity of the films increases to 1−10 S cm^{-1} after being heated to 250 or 350 °C for 1 h (Figure 6). Because these sintered samples show no gate modulation, Hall effect measurements were used to determine their electrical characteristics, yielding *p*-type conductivity, a hole concentration of $5(\pm 2) \times 10^{19}$ cm^{-3} and a hole mobility of 7.5 ± 1.5 cm^2 V^{-1} s^{-1} for NC films treated at 350 °C. The conductivity of films heated to 200 °C is essentially unchanged from that of as-made films, indicating that the transition to high conductivity occurs abruptly between 200 and 250 °C. This is consistent with the above structural studies showing that oleate loss and NC growth commence in earnest in this temperature range. Studies utilizing different annealing regimens have reported somewhat different conduction onsets.[34,35]

(32) Susuki, N.; Sawai, K.; Adachi, S. *J. Appl. Phys.* **1995**, *77*, 1249.
(33) Raab, A.; Springholz, G. *Appl. Phys. Lett.* **2000**, *77*, 2991.
(34) Romero, H. E.; Drndic, M. *Phys. Rev. Lett.* **2005**, *95*, 156801.

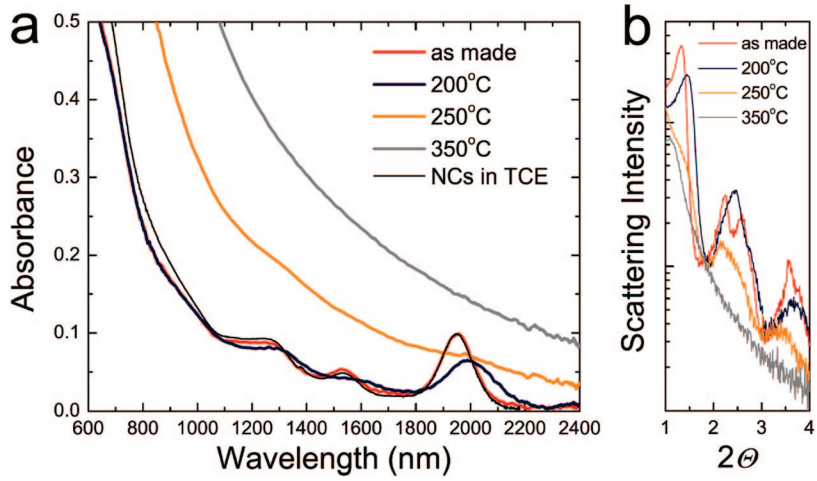

Figure 3. (a) Optical absorption spectra of NC films on sapphire substrates as a function of thermal treatment, acquired with an integrating sphere. The fwhm values of the first exciton peak of the as-made film and the film treated at 200 °C are 49 and 74 meV, respectively. (b) SAXS patterns of the same films on a log-normal scale. NCs with $\lambda_{exciton} = 1950$ nm were used in these measurements. The samples were briefly exposed to air during the measurement process.

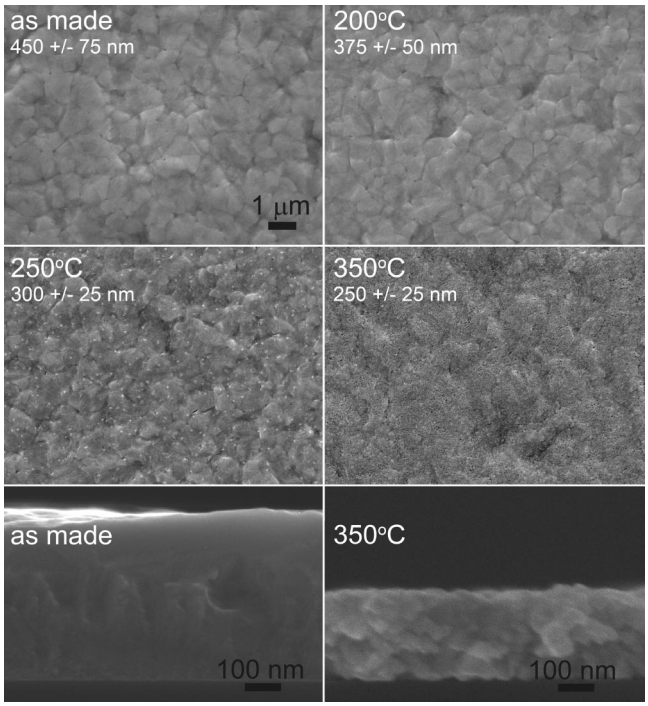

Figure 4. SEM images of NC films on silicon substrates as a function of thermal treatment. The thickness and peak-to-valley roughness of each film are indicated. NCs with $\lambda_{exciton} = 1896$ nm were used for these images.

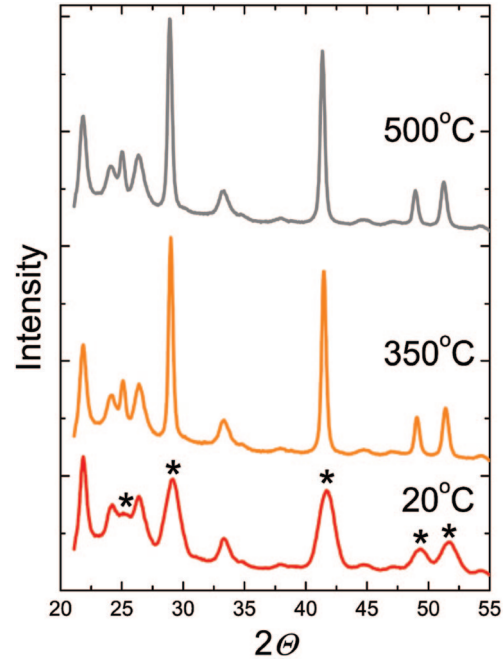

Figure 5. In situ WAXS patterns of a PbSe NC sample at room temperature, 350, and 500 °C in a nitrogen atmosphere. PbSe peaks are labeled with asterisks; unlabeled peaks are due to the polyetheretherketone (PEEK) sample dome used by the in situ diffractometer. NCs with $\lambda_{exciton} = 2020$ nm were used.

Chemical Treatments of PbSe NC Films. We investigated the effects of soaking 450-nm-thick PbSe NC films in solutions of hydrazine, methylamine, or pyridine for 24 h at room temperature. Figure 7 compares WAXS patterns and FTIR spectra of films treated in 1 M hydrazine in acetonitrile, 1 M hydrazine, methylamine or pyridine in ethanol, and pure hydrazine (31 M) and pyridine (12.4 M). Voigt fits to the 220 reflections indicate that the ethanol-based treatments preserve the size of the NCs (7.9 ± 0.2 nm in this case). In contrast, treatments in pure hydrazine or pyridine cause substantial growth of the NCs. Nanocrystal growth can occur by surface diffusion or by dissolution−precipitation, whereby the NCs partially erode to form dissolved species that reprecipitate on neighboring NCs. Hydrazine, which is a stronger reducing agent than pyridine, also converts some of the film to crystalline Pb.

WAXS suggests that treatments in hydrazine in acetonitrile increase the NC diameter by 1−1.5 nm, but this conclusion is inconsistent with our other data, particularly the optical absorption and SAXS measurements (see below). A size increase of 1−1.5 nm should cause the first excitonic transition of these films to red-shift by about ∼100 meV, but the actual red shift is much smaller (12 meV), and smaller than that due to any of the 1 M treatments in ethanol (which show no WAXS peak narrowing). Moreover, NC growth would be expected to

(35) Lifshitz, E.; Brumer, M.; Kigel, A.; Sashchiuk, A.; Bashouti, M.; Sirota, M.; Galun, E.; Burshtein, Z.; Le Quang, A. Q.; Ledoux-Rak, I.; Zyss, J. *J. Phys. Chem. B* **2006**, *110*, 25356.

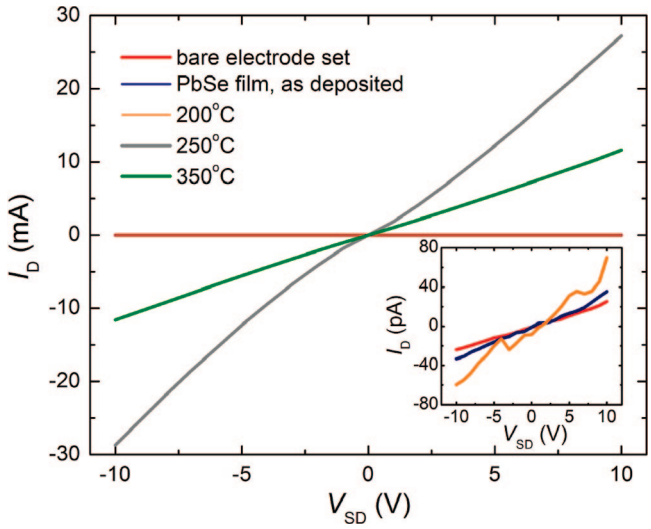

Figure 6. *I*−*V* scans of PbSe films as a function of thermal treatment. Data for a bare substrate are also shown. Inset is a magnified view of the high-resistivity samples, which are indistinguishable in the main plot (L = 23 μm, W = 2100 μm, with an as-made film thickness of ∼300 nm).

substantially alter the SAXS patterns of hydrazine-treated films relative to the other films, but this is not the case. We therefore believe, without being able to otherwise account for the WAXS peak narrowing, that the treatments in hydrazine in acetonitrile do not substantially increase the size of the NCs.

The loss of oleate from the surface of the NCs was quantified by integrating the aliphatic C−H stretch intensity in FTIR spectra, assuming constant oscillator strengths. As Figure 7 shows, soaks in 1 M hydrazine in acetonitrile remove 2−7% of the oleate, while 1 M hydrazine, methylamine, and pyridine in ethanol remove 85−90%, 80−85%, and 18−22% of the oleate, respectively. The hydrazine treatments clearly show a large solvent effect, with the use of ethanol resulting in much greater oleate removal than acetonitrile. In fact, ethanol itself is able to desorb oleate: treatments of as-made films in pure acetonitrile show no loss of oleate, while soaks in pure ethanol remove about 20% (Figure S2). Pyridine in ethanol is therefore no more effective at oleate desorption than ethanol alone. The pure hydrazine and pyridine treatments remove 70% and 95% of the original ligand cap, respectively. Note that, in contrast to ZnSe and CdSe NC films, adsorbed hydrazine, methylamine, and pyridine are not detected on the PbSe NC films by FTIR (Figure S3). Our results show that amines do not have a strong affinity for the surface of the PbSe NCs, at least under the treatment conditions used here.

SAXS was used to monitor changes in the average inter-NC spacing and superlattice order of the films as a function of chemical treatment. In our experimental geometry, SAXS is most sensitive to the top portion of the films (penetration depth of 30−235 nm depending on the angle of incidence and the volume fraction of oleate; see Supporting Information). As-made films show multiple SAXS reflections characteristic of NC superlattices (Figure 8).[4,36] Treatments in pure acetonitrile cause no change in the SAXS patterns, while pure ethanol reduces the NC separation by 5.5 Å, consistent with partial removal of the oleate cap. Surprisingly, treatments with hydrazine in acetonitrile decrease the NC spacing by 8 Å even though less than 7%, and often only 2−3%, of the initial oleate desorbs from these films. In their paper on the effect of acetonitrile-based hydrazine treatments on PbSe NC films,[4] Talapin and

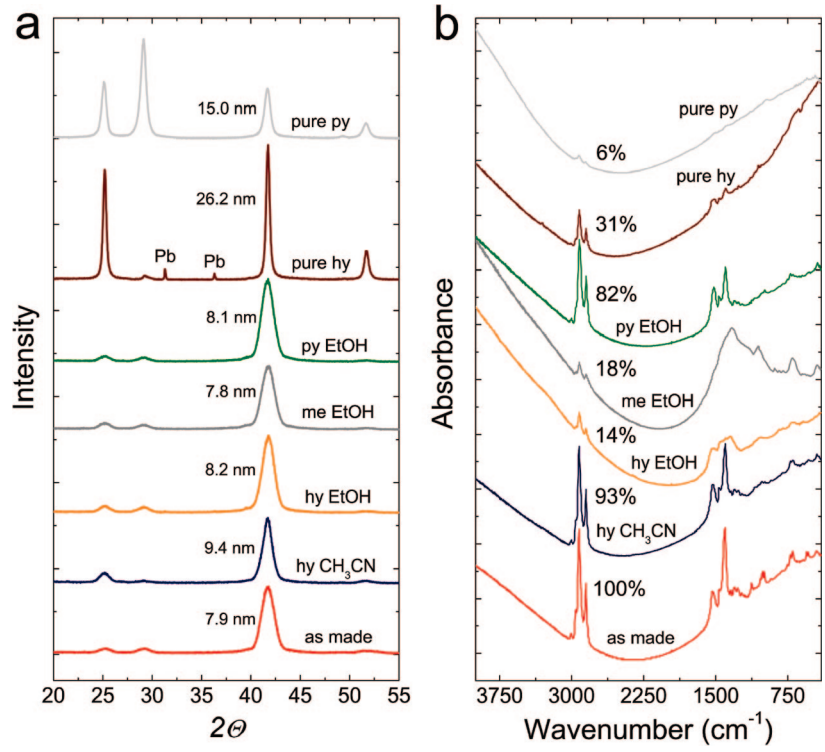

Figure 7. (a) WAXS patterns of chemically treated NC films on sapphire substrates, acquired in air (hy = hydrazine; me = methylamine; py = pyridine). Crystallite sizes calculated using the 220 reflection and assuming zero strain broadening are as indicated (the error for NCs smaller than ∼10 nm is ±2 Å). NCs with $\lambda_{exciton}$ = 2050 nm were used in these measurements. (b) FTIR spectra of films on silicon substrates, acquired in air. The percentage of remaining C−H stretch intensity is shown. Changes in the sloping Fabry−Perot background are due to thinning or cracking of the films. Spectra of films protected from air exposure were nearly identical to those of air-exposed films. NCs with $\lambda_{exciton}$ = 2030 nm were used in these measurements.

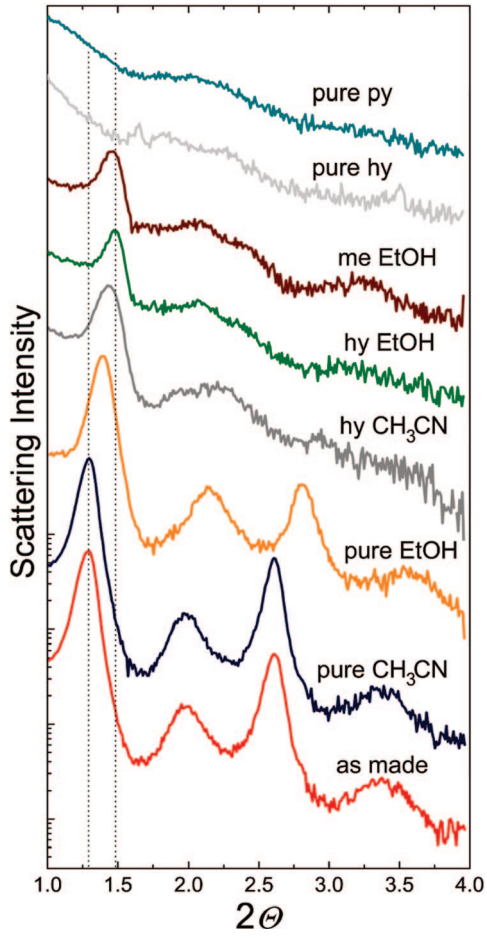

Figure 8. SAXS patterns of chemically treated films on sapphire substrates on a log-normal scale. The traces are offset for clarity. The first peak of the as-made film corresponds to first-order diffraction from close-packed layers of the nanocrystals; shifts toward higher 2Θ indicate a smaller inter-NC spacing in the packing direction along the film normal. The samples were exposed to air during the measurement process. NCs with $\lambda_{exciton}$ = 2030 nm were used in these measurements.

Murray claim, without direct data on oleate loading, that the NC separation decreases because hydrazine replaces oleate on the film surface. Our results instead show that the NCs move closer together despite the fact that hydrazine removes very little oleate from these films. We conjecture that hydrazine causes improved interdigitation of the alkyl chains on neighboring NCs, drawing the NCs closer together without removing oleate. Similar melting and densification of the oleate layer has been observed in PbSe NC films heated under vacuum at 100 °C.[37]

The ethanol-based methylamine and hydrazine treatments remove the most oleate and result in the largest decrease in NC spacing, 9 and 10 Å, respectively. To different degrees, every chemical treatment also ruins the superlattice order of the original films as the layers of NCs buckle and roughen during oleate desorption (or as interdigitation improves). In the case of treatments in pure hydrazine or pyridine, NC growth destroys the superlattice and washes out the SAXS features.

Post-treatment SEM images show varying degrees of film cracking as a result of oleate loss. Treatments in hydrazine in acetonitrile cause little change in the gross morphology of the films (Figure 9). In contrast, ethanol-based treatments result in extensive film cracking, with pyridine causing finer, less interconnected cracks than either hydrazine or methylamine, which is consistent with its smaller degree of oleate loss. Pure

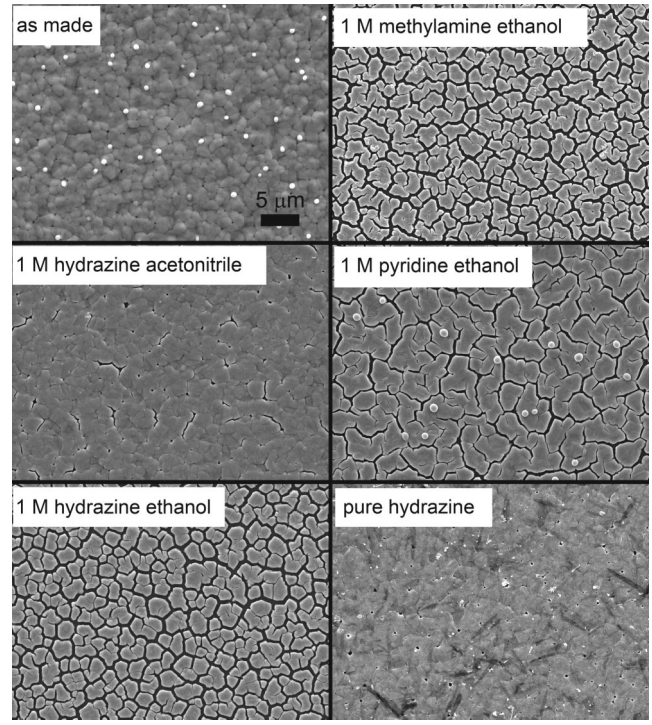

Figure 9. Plan-view SEM images of NC films on silicon substrates as a function of chemical treatment. Small spheres of selenium on the as-made and pyridine-treated films sometimes form after exposure to air for several days. NCs with $\lambda_{exciton}$ = 2030 nm were used in these measurements.

hydrazine and pyridine treatments cause little cracking but rather roughen the surface of the films as a result of NC growth.

XPS was used to measure the surface composition of the chemically treated films (Figure 10 and Table 1). The O 1s spectra of as-made films feature a peak at 531.0 eV and a small shoulder at 532.3 eV, which we assign to the carboxylate group of oleate adsorbed in two different surface sites.[38] In C 1s spectra, the oleate produces a large peak at 284.7 eV due to the alkyl chain and a small peak at 287.7 eV due to the carboxylate moiety. Treating films in 1 M hydrazine in acetonitrile, 1 M pyridine in ethanol, or pure ethanol slightly decreases the intensity of the oxygen and carbon peaks and increases that of the Pb 4f and Se 3d peaks, consistent with the partial removal of oleate observed in FTIR spectra. No nitrogen is detected on films subjected to these three treatments.

XPS indicates that treatments in 1 M methylamine or hydrazine in ethanol strip most of the oleate from the film surface, replacing some of it with adsorbed ethoxide, ethanol, and perhaps other species. The C 1s oleate peaks at 284.6 and 287.6 eV are replaced with four smaller peaks at 284.4 eV, 285.3 eV, 286.7, and 287.6 eV after methylamine treatment. These peaks are assigned to the alkyl chain of residual oleate, the methyl group of adsorbed methylamine,[39] the $-CH_2O-$ group of ethanol and/or ethoxide,[40–42] and the carboxylate group of residual oleate, respectively. Hydrazine-treated films lack the feature at 285.3 eV. There is some variation in the intensity of these peaks between films treated in hydrazine and methylamine and from sample to sample. The O 1s spectra of hydrazine-treated films show a small shoulder at 529.0 eV, a peak at 531.1 eV, and, usually, a third peak at 533.2 eV. Methylamine-treated films always show three peaks, shifted somewhat to 528.5, 530.5, and 533.1 eV. The feature at low binding energy is consistent with atomic oxygen bound as Pb−O or Se−O.[43,44] We assign the peak at 530.5−531.1 eV to residual oleate and

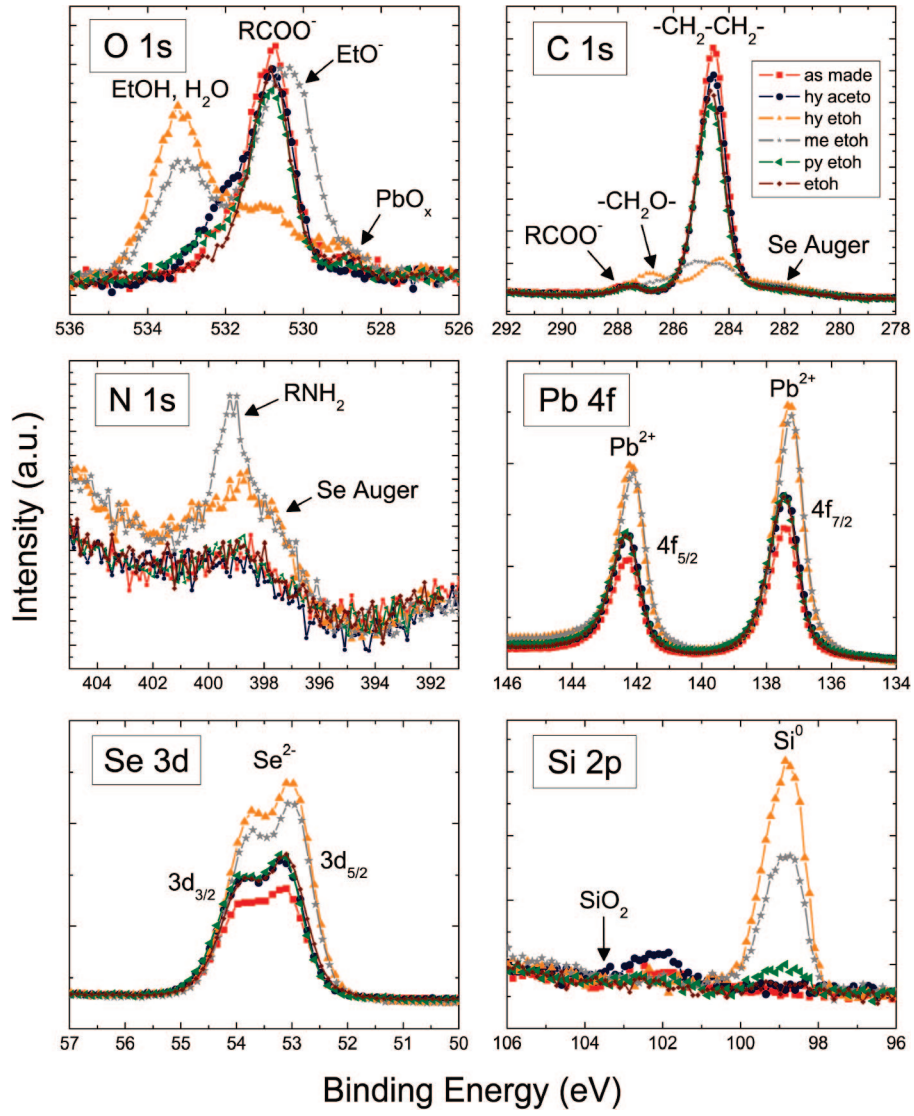

Figure 10. XPS analysis of an as-made film (red squares) and films treated in hydrazine/CH_3CN (blue circles), hydrazine/EtOH (orange triangles), methylamine/EtOH (gray stars), pyridine/EtOH (green triangles), and pure ethanol (brown diamonds). Samples were spin cast onto HF-rinsed silicon substrates, treated for 24 h, and measured without exposure to air. The intensity of the Si 2p signal is roughly proportional to the degree of film cracking (see Figure 9). The Si 2p spectrum also serves to show that the Si substrates are free of SiO_2 and therefore the O 1s peak at 533.1 eV is not due to SiO_2. NCs with $\lambda_{exciton}$ = 1950 nm were used in these measurements.

Table 1. Atomic % Surface Composition of Chemically-Treated PbSe NC Films

treatment	C 1s	O 1s	N 1s[a]	Pb 4f	Se 3d	Si 2p
as made	74.7	6.5	0	9.0	9.0	0.7
hy aceto	69.7	6.8	0	11.3	11.6	0.6
hy EtOH	23.3	12.7	0.3	25.4	27.7	10.6
me EtOH	27.2	16.2	1.6	25.1	24.4	5.5
py EtOH	67.0	6.3	0	12.4	12.9	1.0
EtOH	68.6	6.3	0	12.0	12.2	0.8

[a] Nitrogen values are convolved with a Se LMM Auger line and should be considered upper limits. hy = hydrazine; me = methylamine; py = pyridine.

adsorbed ethoxide.[45] The feature at high binding energy appears sporadically only after ethanol-based treatments and is always accompanied by the $-CH_2O-$ feature at 286.7 eV. We therefore attribute the high-energy O 1s feature to molecular ethanol, although molecular water is another possibility.[42,46–49] A small amount of nitrogen (~1.6 at%) is present on methylamine-treated films, with a peak at ~399 eV corresponding to the NH_2 group of molecular methylamine.[39] The hydrazine-treated films may contain hydrazine at very low coverage (<0.3 at%), but the increased intensity of a selenium Auger line at the same energy makes quantification of nitrogen impossible in this case. The very low concentrations of the nitrogen species explain why they are not observed in the FTIR data.

(36) Murray, C. B.; Kagan, C. R.; Bawendi, M. G. *Annu. Rev. Mater. Sci.* **2000**, *30*, 545.
(37) Mentzel, T. S.; Porter, V. J.; Geyer, S.; MacLean, K.; Bawendi, M. G.; Kastner, M. A. *Phys. Rev. B* **2008**, *77*, 075316.
(38) Wagner, C. D.; Zatko, D. A.; Raymond, R. H. *Anal. Chem.* **1980**, *52*, 1445.
(39) Chen, J. J.; Winograd, N. *Surf. Sci.* **1995**, *326*, 285.
(40) Vohs, J. M.; Barteau, M. A. *Surf. Sci.* **1989**, *221*, 590.
(41) Jayaweera, P. M.; Quah, E. L.; Idriss, H. *J. Phys. Chem. C* **2007**, *111*, 1764.
(42) Weststrate, C. J.; Ludwig, W.; Bakker, J. W.; Gluhoi, A. C.; Nieuwenhuys, B. E. *ChemPhysChem* **2007**, *8*, 932.
(43) Malitesta, C.; Sabbatini, L.; Zambonin, P. G.; Bicelli, L. P.; Maffi, S. *J. Chem. Soc., Faraday Trans. 1* **1989**, *85*, 1685.
(44) Veluchamy, P.; Minoura, H. *Appl. Surf. Sci.* **1998**, *126*, 241.
(45) Alemozafar, A. R.; Madix, R. J. *J. Phys. Chem. B* **2005**, *109*, 11307.

Scheme 1. Amine-Promoted Desorption of Oleate from PbSe{100} in Ethanol

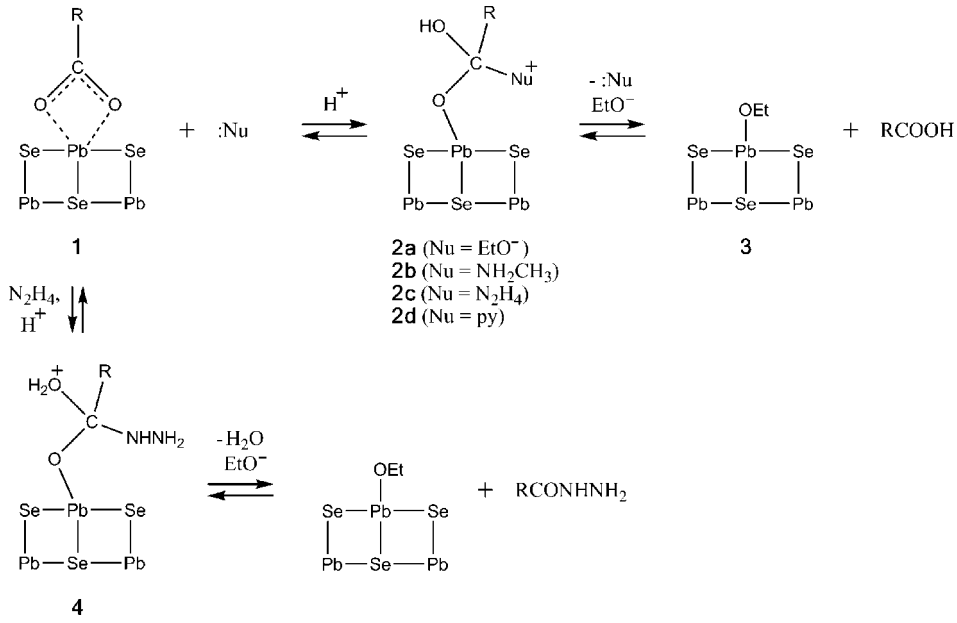

We now turn to the question of why the various chemical treatments remove different amounts of oleate from the NC films. The possibility that the treatment solutions diffuse into the films at drastically different rates must first be considered. We believe that the efficacy of the chemical treatments is not determined by diffusion, for two reasons. First, both the pure solvents and the amine solutions thoroughly wet the NC films. Second, treatments in 0.01 M solutions of thiols in either acetonitrile[50] or ethanol strip ~100% of the oleate from the films in 1−2 min. These observations strongly suggest that the treatment solutions rapidly permeate the NC films and that oleate desorption is determined by surface reaction equilibria rather than the variable extent of solution diffusion into the films.

The large solvent effect evident in the hydrazine treatments provides insight into the mechanism of oleate removal. Because ethanol is protic and therefore much more acidic than acetonitrile ($pK_a = 15.9$, compared to ~25 for acetonitrile), it facilitates desorption of oleate in the form of oleic acid. Oleic acid was the only oleate desorption product detected by FTIR and NMR spectroscopy when the NCs were treated in pure ethanol or solutions of methylamine or pyridine in ethanol, while no oleate derivatives were found after treatment of NCs in pure acetonitrile. We believe that the desorption reaction in pure ethanol involves the substitution of oleate by ethoxide, as shown in Scheme 1, where oleate is drawn chelated to a single Pb atom on the PbSe{100} surface (**1**).[51] This reaction may occur via the nucleophilic addition of ethoxide to the carboxylate group, followed by protonation, transfer of ethoxide to the NC surface, and loss of oleic acid. Nucleophilic addition serves to activate

Scheme 2. Dissociation of the Nanocrystal Oleate Complex on PbSe{100}

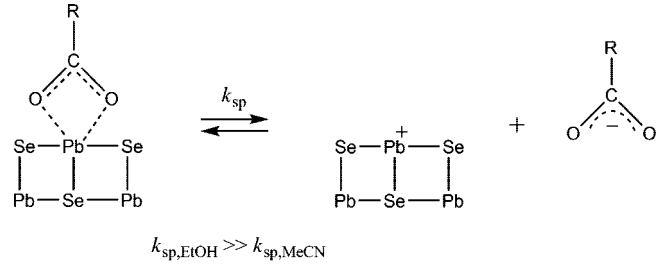

oleate toward protonation and desorption by forming a tetrahedral intermediate (**2**) featuring a strongly basic oxygen atom. In this picture, the addition of methylamine ($pK_b = 3.4$) or hydrazine ($pK_b = 5.8$) to ethanol increases the concentration of nucleophiles (both the ethoxide and the amine itself), thereby affecting greater oleate removal than ethanol alone. Pyridine ($pK_b = 8.8$) has little impact beyond pure ethanol ostensibly because it is a weaker base and bulkier nucleophile than either methylamine or hydrazine. A mixture of desorbed oleic acid and oleic hydrazide was found by FTIR and NMR after treatments in hydrazine in ethanol. The hydrazide may form via intermediate (**4**).

Hydrazine treatments in acetonitrile remove little oleate because of the scarcity of free protons in this solvent. We note that while acetonitrile-based hydrazine treatments remove 2−7% of the oleate from PbSe NC films, they remove 30−40% of the oleate from ZnSe and CdSe NC films, to which hydrazine adsorbs strongly (Figure S3). Dissociative chemisorption of hydrazine or methylamine on ZnSe and CdSe can directly displace oleate as oleic acid.

A second oleate desorption mechanism that may be significant is the ionic dissociation of the NC oleate salt (Scheme 2). Oleate salts are practically insoluble in acetonitrile but moderately soluble in ethanol (>0.01 M for sodium oleate). If the solubility product of the bound oleate, k_{sp}, is appreciable in ethanol at room temperature, some fraction of the free oleate will be protonated by ethanol and some fraction of the vacant Pb surface sites will be passivated by ethoxide or another nucleophile from

(46) Herman, G. S.; Dohnálek, Z.; Ruzycki, N.; Diebold, U. *J. Phys. Chem. B* **2003**, *107*, 2788.
(47) Dupin, J.-C.; Gonbeau, D.; Vinatier, P.; Levasseur, A. *Phys. Chem. Chem. Phys.* **2000**, *2*, 1319.
(48) Andersson, K.; Nikitin, A.; Pettersson, L. G. M.; Nilsson, A.; Ogasawara, H. *Phys. Rev. Lett.* **2004**, *93*, 196101.
(49) Weststrate, C. J.; Ludwig, W.; Bakker, J. W.; Gluhoi, A. C.; Nieuwenhuys, B. E. *J. Phys. Chem. C* **2007**, *111*, 7741.
(50) Luther, J. M.; Law, M.; Song, Q.; Perkins, C. L.; Beard, M. C.; Nozik, A. J. *ACS Nano* **2008**, *2*, 271.
(51) This oleate adsorption geometry is supported by FTIR data and density function theory calculations; unpublished results.

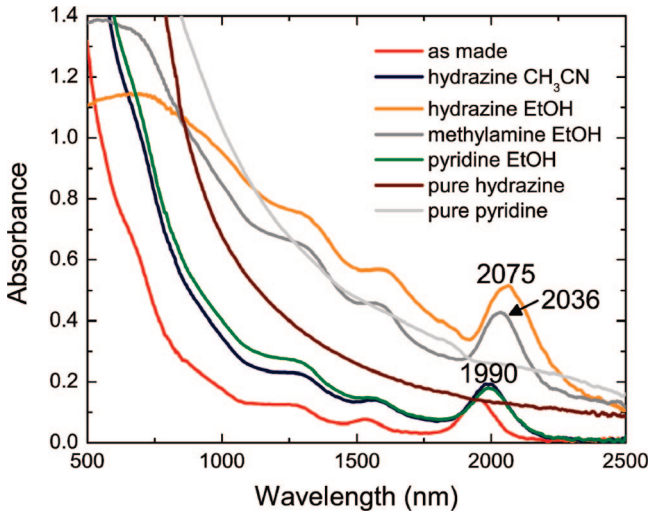

Figure 11. Optical absorption spectra of chemically treated films on sapphire substrates, acquired with an integrating sphere in an air-free measurement cell. Spectra are not offset. The fwhm of the first exciton peak of the as-made film is 50 meV, increasing to 52−53 meV for the treated films. The absorbance of several of the films rolls off at bluer wavelengths because light is transmitted through cracks in these films (see Figure 10). Accurate measurements require that the samples be protected from air because the films oxidize in air at different rates (see Figure S5). NCs with $\lambda_{exciton} = 1950$ nm were used in these measurements.

the solution. In this picture, the addition of an amine base to ethanol increases the concentration of ethoxide available to bind to vacant Pb sites, thereby shifting the equilibrium toward desorbed oleate and oleic acid. In contrast, adding hydrazine to acetonitrile only slightly increases the amount of oleate removed from the NC film because k_{sp} is much smaller in acetonitrile.

These desorption schemes are largely consistent with our FTIR, NMR and XPS data, the solvent effect, and the negligible coverage of adsorbed amines on the PbSe NC films, which rules out amine chemisorption in the mechanism. The evidence for adsorbed ethoxide (**3**) is admittedly weak. It is strongest for films treated in methylamine, which show alkoxide oxygen by XPS (Figure 10) and C−O stretching at 1050−1100 cm^{-1} in FTIR spectra[52] (Figure 7B).

Removal of the insulating oleate and the concomitant decrease in the nanocrystal spacing triggers a Mott-type insulator to conductor transition[53] that has a marked effect on the optical absorption of the NC films. Figure 11 shows that treatments with hydrazine in acetonitrile or pyridine in ethanol cause the first exciton of the NCs to red-shift by 12 meV (40 nm). At the same time, absorbance is enhanced across the spectrum such that the film color changes from light brown to dark brown. Treatments in pure ethanol produce very similar absorbance shifts (Figure S2). The other treatments cause more dramatic changes. Hydrazine and methylamine in ethanol red-shift the first exciton by 27 meV (86 nm) and 38 meV (125 nm), respectively, and increase the absorbance sufficiently to change the color of the films to a deep gray. As expected, pure hydrazine or pyridine treatments obliterate the NC excitonic features and yield a bulk-like absorption spectrum.[32] These absorbance increases and red shifts arise from a combination of (*i*) an increased dielectric constant of the medium surrounding the NCs after oleate loss, which boosts oscillator strengths; (*ii*) increased dipole−dipole (radiative) coupling between NCs; and (*iii*) a

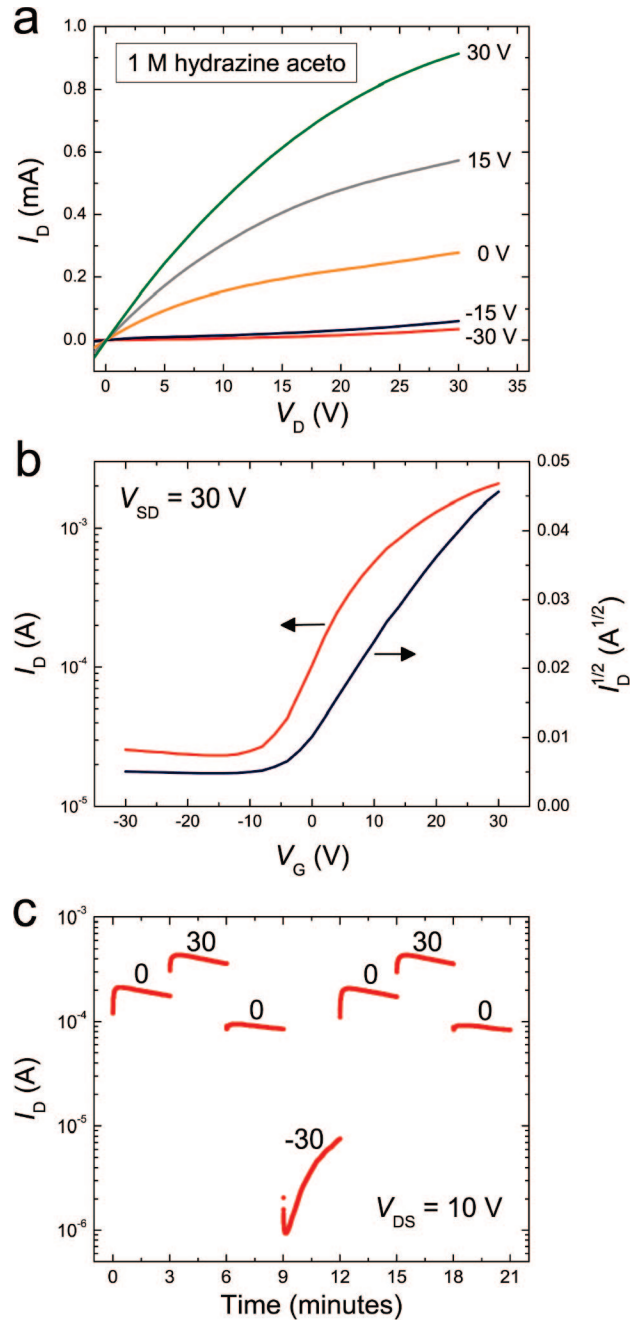

Figure 12. (a) Output and (b) transfer characteristics of a PbSe NC film activated with hydrazine in acetonitrile for 24 h. The plot of $I_D^{1/2}$ was used to calculate the device mobility according to the gradual channel approximation.[54] (c) Time dependence of I_D as a function of V_G in the dark for a different device. The gate voltage was cycled between −30 V and +30 V using 30 V steps every 3 min. $V_{DS} = 10$ V. ($L = 23$ μm, $W = 2100$ μm, $t = 175 \pm 25$ nm).

greater wave function overlap between NCs (nonradiative electronic coupling).[50] NC growth plays a major role only in the pure hydrazine and pyridine treatments.

We briefly studied the effect of aging the chemically treated NC films in ambient laboratory conditions. After four days on the benchtop, the first exciton absorptions of the films in Figure 11 lost intensity and blue-shifted by 40−65 meV (120−192 nm), indicating a reduction in internanocrystal coupling and nanocrystal size (Figure S5). WAXS shows that aging as-made films for 3 weeks in air reduces the crystalline diffraction volume and decreases the NC diameter by ∼0.7 nm (Figure S6). In

(52) Yee, A.; Morrison, S. J.; Idriss, H. *J. Catal.* **2000**, *191*, 30.
(53) Remacle, F. *J. Phys. Chem. A* **2000**, *104*, 4739.

Table 2. Structural and Electrical Results from Chemically Treated PbSe NC Films[a]

treatment	% oleate removed	Δ NC spacing, Å	$\Delta h\nu_{exciton}$, meV	σ, S cm^{-1}	type	mobility, cm^2 V^{-1} s^{-1}	I_{ph}/I_{dark}
hy aceto	2–7	8	10–13	5×10^{-3}	n	0.5–1.2	2–3
hy EtOH	85–90	10	36–39	5×10^{-2}	n	n/a	2–3
me EtOH	80–90	9	25–30	1×10^{-4}	p	n/a	2
py EtOH	15–20	n/a	10–14	5×10^{-3}	p	n/a	2–3
EtOH	15–20	5.5	12	1×10^{-2}	p	n/a	2–3

[a] Six to ten films of each type were measured. Conductivity (σ) and mobility were measured in the dark. The photoconductivity ratio (I_{ph}/I_{dark}) was measured at $V_{SD} = 10$ V and $V_G = 0$ under 300 mW cm^{-2} broadband tungsten illumination ($L = 23$ μm).

addition, the substantially lower SAXS intensity of aged films shows that the oxidation process disorders the films. The NC spacing may also increase slightly as the films age. A proper investigation of the effects of air exposure on these NC films requires a separate study.

Electrical Measurements of Chemically Treated Films. Using a field effect transistor (FET) geometry, we measured NC films treated in 1 M hydrazine in acetonitrile, 1 M hydrazine, methylamine or pyridine in ethanol, or pure ethanol. The key structural and electrical findings from these chemically treated films are summarized in Table 2.

Treating the PbSe NC films in solutions of hydrazine in acetonitrile yields conductive, *n*-type FETs with high electron mobility and decent I_{ON}/I_{OFF} values, as shown previously by Talapin and Murray.[4] Figure 12 shows the output and transfer characteristics of a device with a mobility in the saturation regime of 0.97 cm^2 V^{-1} s^{-1}, an on/off ratio of 80 ($V_D = 30$ V) and a conductivity in the on-state of 4×10^{-2} S cm^{-1}. A series of devices yielded saturation mobilities in the range 0.5−1.2 cm^2 V^{-1} s^{-1} and on/off ratios as high as 330 (at $V_D = 30$ V). We confirmed that the hydrazine-treated films can be rendered *p*-type by heating them to 125 °C in N_2 for several hours; re-exposure to hydrazine for several minutes switches them back to *n*-type, as previously reported.[4] The heat treatment probably removes the very small amount of hydrazine that is undoubtedly adsorbed to these films. Adsorption of several hydrazine molecules per nanocrystal would be sufficient to dope the films yet below the detection limit of our FTIR and XPS probes.

The films treated in hydrazine in acetonitrile show additional behavior not reported previously. Exposing hydrazine-activated *n*-FETs to laboratory air for 5 min results in a 10-fold increase

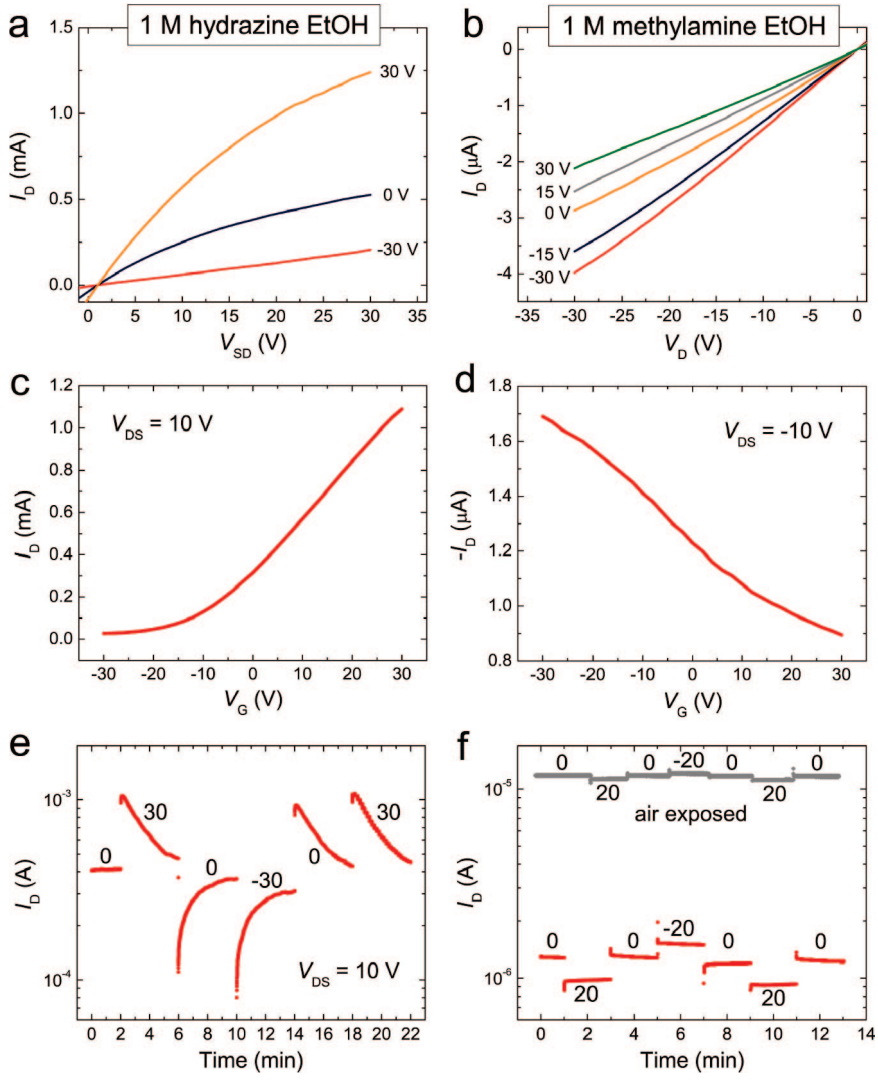

Figure 13. (a and b) Output and (c and d) transfer characteristics of PbSe NC films treated with hydrazine or methylamine in ethanol for a total of 24 h. (e and f) Time dependence of I_D as a function of V_G in the dark. A time trace for the methylamine-treated film after exposure to air for 5 min is also shown. $V_{DS} = 10$ V. See Figure S9 for SEM images of a hydrazine-treated device ($L = 23$ μm, $W = 2100$ μm, $t = 80 \pm 10$ nm).

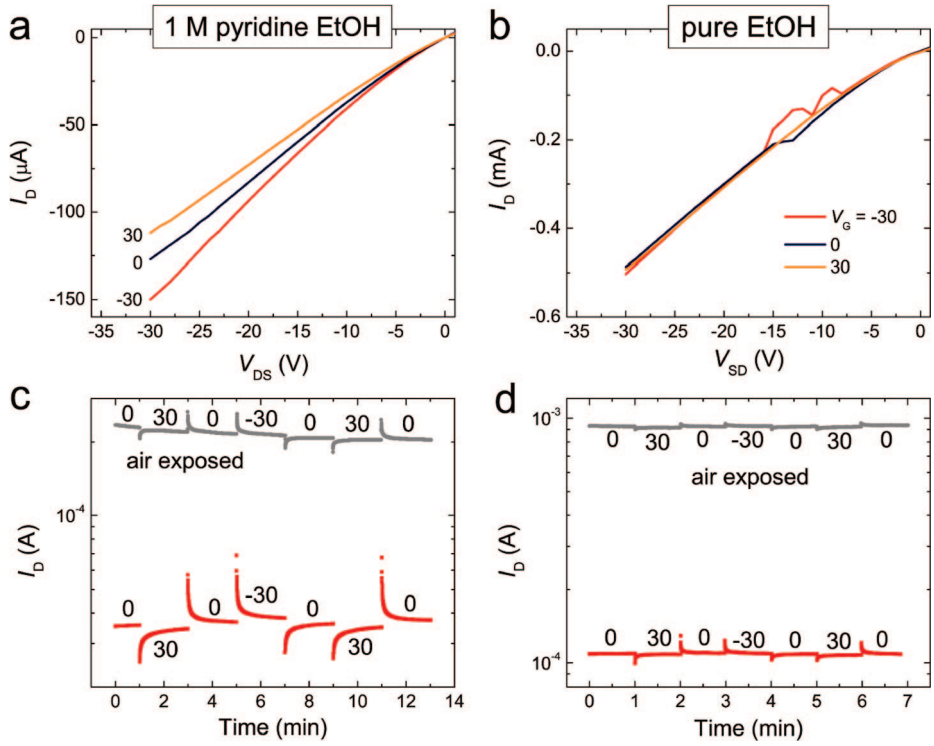

Figure 14. (a and b) Output characteristics of PbSe NC films treated with pyridine in ethanol or pure ethanol for a total of 24 h. (c and d) Time dependence of I_D as a function of V_G in the dark. Time traces for the films after air exposure are also shown. $V_{DS} = 10$ V ($L = 23$ μm, $W = 2100$ μm, $t = 80 \pm 10$ nm).

in conductivity and the loss of gate modulation, which is fully reversible upon subsequent hydrazine treatment (Figure S7). In addition to this extreme air sensitivity, our hydrazine-treated FETs suffer from threshold voltage shifts in response to gate voltage cycling, with particularly large shifts occurring during the first few V_G sweeps (Figure S8). Furthermore, time traces show that I_D exhibits transients upon changes in V_G, particularly when V_G is stepped to large negative values (Figure 12c). This behavior is probably caused by trap charging and/or charge redistribution within the NC film or at the NC/oxide interface in response to steps in the applied gate field. Nanocrystal films should be especially susceptible to such charging because they contain a large number of grain boundaries and possible surface traps. As a check on the FET substrates and setup, we found that FETs made from spin-coated poly(3-hexylthiophene) (P3HT) exhibit stable I_D switching with changes in V_G.[50] Furthermore, modifying the surface of the gate oxide via dehydrating heat treatments or hexamethyldisilazane (HMDS) functionalization prior to NC deposition did not affect the I_D transients, which suggests that the charging occurs within the NC film itself rather than in or on the oxide. This is true of all of the chemically treated films discussed here.

Soaking films in 1 M hydrazine in ethanol rather than acetonitrile results in *n*-type FETs of higher conductivity (5×10^{-2} S cm^{-1}) but poorer gate modulation, with on/off ratios of only 5−15 for gate swings of ±30 V (Figure 13a,c). Moreover, the I_D of these devices decays rapidly after a change in V_G such that the gate field is largely screened within a few minutes (Figure 13e). The combination of high conductivity, weak gating, and pronounced I_D transients is consistent with a high density of free electrons and surface traps in these NC films, both conceivably created by oleate removal and the adsorption of trace amounts of hydrazine during the ethanol-based hydrazine treatments. The large carrier density reduces the ability of the gate field to enhance/deplete the transistor channel and, combined with the large trap density, results in marked I_D transients.

Methylamine treatments yield *p*-FETs of moderate conductivity (10^{-4} S cm^{-1}), weak gate modulation, and relatively stable drain currents (Figure 13b, d, and f). The very different behavior of PbSe NC FETs prepared with ethanolic methylamine and ethanolic hydrazine are striking considering their similar FTIR and XPS spectra and expected surface chemistry. Hole doping is surprising for methylamine, which, like hydrazine, is a nucleophile and reducing agent. However, the doping of NC solids by surface species is likely a sensitive function of the mixture of adsorbates present on the surface and the energy levels of the surface states. It is possible that methylamine, one of its surface reaction products, or an impurity in the methylamine solution passivates surface traps differently than the hydrazine solution and dopes the films *p*-type.

Treatments in pyridine in ethanol or pure ethanol produce *p*-FETs characterized by rapid I_D transients and a dark conductivity of 5×10^{-3} S cm^{-1} and 10^{-2} S cm^{-1}, respectively (Figure 14). Transfer data were not collected for these devices because of their particularly fast screening of the gate field, which we again attribute to charge trapping. Note that while these two films appear identical in FTIR, XPS, and XRD, pyridine-treated FETs are 3−6 times less conductive than ethanol-treated FETs. This reemphasizes how sensitive the electrical properties of NC films can be to variations in adsorbate composition. It is striking that a simple treatment in ethanol, which strips only 20% of the oleate and reduces the NC spacing by only 5.5 Å, produces such conductive NC films. We plan to use temperature-

(54) Kagan, C. R.; Andry, P. *Thin Film Transistors*; Marcel Dekker: New York, 2003.

dependent electrical measurements to better understand the nature of charge transport in these chemically treated NC solids.

Exposing any of the chemically treated films to air for 5 min causes a 10-fold increase in conductivity and a switch to *p*-type conduction with rapid I_D transients and $I_{ON}/I_{OFF} \approx 1$. The conductivity jump is probably due to adsorbed oxygen, hydroxyl, and water that dope the film and narrow the tunneling barrier between NCs. It is likely that longer air exposures convert the films to insulating PbSe/PbO_{1-x} or PbSe/$PbSeO_3$ core−shell NC solids.

Conclusions

PbSe nanocrystal films are of interest as the active layer of solar cells that produce very large currents by the process of multiple exciton generation. We have described the use of heat treatments and amine-based chemical treatments that convert oleate-capped NC films from insulators to conductors. Heat treatments cause NC sintering before substantial oleate loss and result in very conductive, *p*-type polycrystalline films. Treatments in pure hydrazine or pyridine strip much of the oleate but also cause uncontrolled NC growth. Soaking films in 1 M solutions of hydrazine, methylamine, or pyridine in ethanol removes between 20% and 90% of the oleate while preserving the size of the NCs. These films show disparate electrical behavior despite quite similar FTIR and XPS spectra and X-ray scattering patterns, which highlights the importance of subtle differences in adsorbate composition. Treatments in hydrazine in acetonitrile remove very little oleate yet decrease the NC separation by 8 Å and yield high-mobility *n*-type FETs. The surface coverage of amines on the chemically treated films is very low. In addition, the presence of pronounced I_D transients suggests that a large density of surface traps exists within most of the amine-treated NC films.

From a solar cell fabrication perspective, postdeposition treatments of NC films are problematic because volume loss tends to cause macroscopic cracks that short circuit the cell when a metal electrode is deposited onto the film. A second round of NC deposition and treatment rarely eliminates all of these shorts. Predeposition ligand exchanges risk NC aggregation and ripening, but the self-assembly of NCs stabilized by short-chain organic ligands (*n*-butylamine, for example) can produce crack-free and conducting NC superlattices in a single step.[11] Another, perhaps more promising, way to make NC films for solar applications is layer-by-layer assembly, in which thick films are built up by multiple cycles of NC deposition and chemical treatment.[50] Adding 1−10 NC monolayers per cycle prevents the accumulation of stress in the growing film, thereby avoiding cracks and pinholes, maximizing mechanical strength, and, in principle, minimizing the positional disordering of the NCs.

Acknowledgment. We thank D. Ginley and group for use of the glove boxes, L. Gedvilas for assistance with FTIR, M. Page for wafer preparation, B. Rupert for discussions, H. Pilath for help with DSC, and P. Parilla for a kind introduction to SAXS and in situ WAXS measurements. Funding is provided by the U.S. Department of Energy, Office of Basic Energy Sciences, Division of Chemical Sciences, Biosciences and Geosciences.

Supporting Information Available: TGA-DSC data, FTIR and UV−vis spectra of films treated in the pure solvents, comparative FTIR data from ZnSe and CdSe NC films, the time dependence of oleate removal, data on film oxidation, additional analysis of certain NC FETs, and a discussion of our use of small-angle X-ray scattering. This material is available free of charge via the Internet at http://pubs.acs.org.

JA800040C